Inflammation-induced desmoglein-2 ectodomain shedding compromises the mucosal barrier

Ryuta Kamekura[a,b], Porfirio Nava[a,c], Mingli Feng[a,d], Miguel Quiros[a,d], Hikaru Nishio[a], Dominique A. Weber[a], Charles A. Parkos[a,d], and Asma Nusrat[a,d]

[a]Epithelial Pathobiology and Mucosal Inflammation Research Unit, Department of Pathology and Laboratory Medicine, Emory University, Atlanta, GA 30322; [b]Department of Human Immunology, Research Institute for Frontier Medicine, Sapporo Medical University School of Medicine, Sapporo 0608556, Japan; [c]Department of Physiology, Biophysics, and Neuroscience, Center for Research and Advanced Studies, Mexico DF 07360, Mexico; [d]Department of Pathology, University of Michigan, Ann Arbor, MI 48109

ABSTRACT **Desmosomal cadherins mediate intercellular adhesion and control epithelial homeostasis. Recent studies show that proteinases play an important role in the pathobiology of cancer by targeting epithelial intercellular junction proteins such as cadherins. Here we describe the proinflammatory cytokine-induced activation of matrix metalloproteinase 9 and a disintegrin and metalloproteinase domain–containing protein 10, which promote the shedding of desmosomal cadherin desmoglein-2 (Dsg2) ectodomains in intestinal epithelial cells. Epithelial exposure to Dsg2 ectodomains compromises intercellular adhesion by promoting the relocalization of endogenous Dsg2 and E-cadherin from the plasma membrane while also promoting proliferation by activation of human epidermal growth factor receptor 2/3 signaling. Cadherin ectodomains were detected in the inflamed intestinal mucosa of mice with colitis and patients with ulcerative colitis. Taken together, our findings reveal a novel response pathway in which inflammation-induced modification of columnar epithelial cell cadherins decreases intercellular adhesion while enhancing cellular proliferation, which may serve as a compensatory mechanism to promote repair.**

Monitoring Editor
Alpha Yap
University of Queensland

Received: Mar 17, 2015
Revised: Jul 20, 2015
Accepted: Jul 21, 2015

INTRODUCTION

Epithelial cells form a selective barrier that separates the external environment from the underlying tissue compartments. In the intestine, where epithelial cell turnover occurs within 1 wk, barrier properties of the columnar epithelium are maintained by intercellular junctions, which include tight junctions, adherens junctions, and desmosomes. In addition to controlling adhesion, proteins in these intercellular junctions also regulate epithelial homeostasis through the processes of cellular proliferation, migration, differentiation, and apoptosis (Allen *et al.*, 1996; Dusek *et al.*, 2006; Dusek and Attardi, 2011; Getsios *et al.*, 2009; Marchiando *et al.*, 2010; Nava *et al.*, 2013).

Along with E-cadherin in the adherens junction, the desmosomal cadherin family members desmoglein and desmocollin mediate cell–cell adhesion in the epithelium. Desmoglein and desmocollin constitute the adhesive core of desmosomes, anchoring intermediate filaments to sites of intercellular adhesion (Getsios *et al.*, 2004; Green and Simpson, 2007). Both proteins are required for de novo desmosome formation in cells that lack cadherin-based junctions (Tselepis *et al.*, 1998; Schlegel *et al.*, 2010). In humans, four desmoglein isoforms (Dsg1–4) and three desmocollin isoforms (Dsc1–3) are expressed in a tissue-specific and differentiation-specific manner (Holthofer *et al.*, 2007). Although stratified epithelia in the epidermis express multiple desmosomal cadherin isoforms, only desmoglein-2 (Dsg2) and desmocollin-2 (Dsc2) are expressed in the simple columnar epithelium of the human intestine (Holthofer *et al.*, 2007).

This article was published online ahead of print in MBoC in Press (http://www.molbiolcell.org/cgi/doi/10.1091/mbc.E15-03-0147) on July 29, 2015.

Address correspondence to: Asma Nusrat (anusrat@umich.edu).

Abbreviations used: ADAM, a disintegrin and metalloproteinase domain–containing protein; Dsc, desmocollin; Dsg, desmoglein; EC, extracellular domain; IBD, inflammatory bowel disease; IEC, intestinal epithelial cell; IFN, interferon; IL, interleukin; MAPK, mitogen-activated protein kinase; MMP, matrix metalloproteinase; mTOR, mammalian target protein of rapamycin; sDsc2, soluble Dsc2; sDsg2, soluble Dsg2; sE-cadherin, soluble E-cadherin; DSS, dextran sulfate sodium; EdU, 5-ethynyl-2′-deoxyuridine; EGFR, epidermal growth factor receptor; GAPDH, glyceraldehyde 3-phosphate dehydrogenase; HER, human epidermal growth factor receptor; JAM-A, junctional adhesion molecule-A; MEK, MAPK kinase; PBS, phosphate-buffered saline; SIRP, signal regulatory protein; TAPI, TNF protease inhibitor; TNF, tumor necrosis factor.

Recent studies show that several proteinases target epithelial intercellular junction proteins during physiological maturation and in pathological states such as inflammation and cancer (Maretzky *et al.*, 2008; Sewpaul *et al.*, 2009; David and Rajasekaran, 2012). The cleavage products of these junction proteins have biological properties that influence the delicate balance of epithelial homeostasis, thereby contributing to disease pathogenesis (Brennan *et al.*, 2007; Kolegraff *et al.*, 2011a,b; Kamekura *et al.*, 2014). Epithelial homeostasis is also perturbed by the proinflammatory cytokines interferon-γ (IFN-γ), interleukin-1β (IL-1β), and tumor necrosis factor-α (TNF-α), which are released into the epithelial milieu during mucosal inflammation, such as in inflammatory bowel disease (IBD; Rogler and Andus, 1998; Nava *et al.*, 2010; Koch and Nusrat, 2012). A functional role for intercellular junction protein cleavage products in cancer progression has also been reported (Kuefer *et al.*, 2003; Najy *et al.*, 2008; Brouxhon *et al.*, 2014a). However, the biological effect and mechanisms by which cadherin cleavage fragments influence intestinal epithelial homeostasis during mucosal inflammation remain unclear (Dusek *et al.*, 2006; Nava *et al.*, 2007; Steck *et al.*, 2011).

Here we report that IL-1β and TNF-α induce Dsg2 cleavage in intestinal epithelial cells (IECs), generating 25- and 100-kDa extracellular domain (EC) fragments. The use of epitope-mapped antibodies reveals the identity of the cleaved fragments as Dsg2 EC1 and Dsg2 EC1–4. Our results showed that proinflammatory cytokine-induced cleavage of Dsg2 ectodomains is mediated by matrix metalloproteinase 9 (MMP9) and a disintegrin and metalloproteinase domain–containing protein 10 (ADAM10). These Dsg2 ectodomains influence intercellular adhesion and epithelial proliferation by promoting relocalization of cadherin from the plasma membrane. In addition, Dsg2 EC1 and EC1–4 enhance IEC proliferation by activating human epidermal growth factor receptor family members HER2 and 3, which activate downstream signaling through the Akt/mammalian target protein of rapamycin (mTOR) and mitogen-activated protein kinase (MAPK) pathways. These findings reveal the biological mechanisms by which Dsg2 cleavage during mucosal inflammation influences intestinal epithelial homeostasis. Thus, interfering with the generation and/or function of these cleavage products may strengthen the epithelial barrier during mucosal inflammation.

RESULTS

Proinflammatory cytokines promote cleavage and shedding of cadherins in intestinal epithelial cells

Previous studies demonstrated that proinflammatory cytokines released during mucosal inflammation alter epithelial homeostasis and barrier function (Rogler and Andus, 1998; Bruewer *et al.*, 2003; Maretzky *et al.*, 2005, 2008; Simpson *et al.*, 2010; Koch and Nusrat, 2012). To determine whether proinflammatory cytokines induce cadherin cleavage in IECs, we used epitope-mapped monoclonal antibodies that recognize extracellular domains of Dsg2 (AH12.2, EPR6767; Figure 1A), Dsc2 (7G6), and E-cadherin (HECD-1) to detect cadherin fragments in the supernatants of T84 human IECs treated with IFN-γ, IL-1β, and TNF-α. The specificity of Dsg2 antibodies was confirmed by immunoblotting (Supplemental Figure S1, A and B). Figure 1B shows that exposure to IL-1β and TNF-α promoted shedding of the soluble 25- and 100-kDa ectodomain fragments of Dsg2 (sDsg2), soluble 80-kDa fragments of Dsc2 (sDsc2), and soluble 80-kDa fragments of E-cadherin (sE-cadherin) into the culture medium. In addition, sDsc2 and sE-cadherin, but not sDsg2, were detected after IFN-γ treatment. We found that the shedding of sDsg2, sDsc2, and sE-cadherin increased with higher concentrations of IL-1β (Figure 1C). After treatment with 20 ng/ml IL-1β, cadherin ectodomain fragments were detected in the culture supernatants within 1 h, with maximum shedding observed 6 h after treatment (Figure 1D). Similar dose- and time-dependent shedding of Dsg2, Dsc2, and E-cadherin was observed after TNF-α treatment (Figure 1, E and F). To complement the in vitro studies, we analyzed the release of Dsg2, Dsc2, and E-cadherin fragments in ex vivo mouse colonic mucosa cultures and found that exposure to IL-1β and TNF-α increased sDsg2, sDsc2, and sE-cadherin by 2.4- to 7.0-fold in the culture supernatants, as assessed by densitometry (Figure 1G).

MMP9 and ADAM10 cleave cadherin ectodomains of intestinal epithelial cells

Proinflammatory cytokines have been reported to activate MMPs and ADAM proteins (Medina and Radomski, 2006; Santana *et al.*, 2006; Pruessmeyer *et al.*, 2010), which cleave epithelial junction proteins in pathological states such as inflammation and cancer (Maretzky *et al.*, 2008; Sewpaul *et al.*, 2009; David and Rajasekaran, 2012). MMP activity and/or expression are increased in the intestinal mucosa of individuals with IBD and in mouse models of intestinal mucosal inflammation (Medina *et al.*, 2003; Santana *et al.*, 2006). Therefore we investigated the role of MMP and ADAM proteins in mediating the cleavage of IEC cadherins by pretreating IECs with TNF protease inhibitor 2 (TAPI-2), an inhibitor of MMPs and ADAM17, before incubation with IL-1β and TNF-α. Our results showed that TAPI-2 inhibited the shedding of sDsg2, sDsc2, and sE-cadherin induced by treatment with IL-1β, TNF-α, or an IL-1β/TNF-α cocktail (Figure 2, A and B, and Supplemental Figure S1C).

Because previous studies showed that IL-1β and TNF-α, but not IFN-γ, increase the activity of MMP2 and 9 (Medina *et al.*, 2003; Medina and Radomski, 2006; Santana *et al.*, 2006), we investigated the role of these proteinases in the control of cadherin cleavage. The results of gelatin zymography revealed higher levels of MMP9 activity in the supernatants of IECs incubated with IL-1β and TNF-α but not in IECs incubated with IFN-γ. However, compared with MMP9, increase in MMP2 activity was observed only with IL-1β (Figure 2C).

We also analyzed ex vivo colonic mucosa cultures derived from healthy mice and mice with dextran sulfate sodium (DSS)–induced colitis. Consistent with results obtained using the in vitro cell cultures, MMP2 and 9 activities and protein levels were elevated in supernatants of colonic mucosal cultures derived from colitic mice (Figure 2D and Supplemental Figure S1D). To confirm the role of these proteinases in the cleavage of cadherin ectodomains, we treated T84 IEC cultures with pharmacologic inhibitors of MMP2 and 9. Immunoblot analysis of supernatants obtained from TNF-α–treated IECs revealed that inhibition of MMP9, but not inhibition of MMP2, decreased the release of sDsg2, sDsc2, and sE-cadherin (Figure 2E). Inhibition of both MMP2 and 9 did not produce a synergistic effect, suggesting the influence of an additional proteinase in this process (Figure 2E). A previous study showed that the membrane-bound metalloproteinase ADAM10 targets Dsg2 (Bech-Serra *et al.*, 2006); therefore we examined whether ADAM10 contributes to cytokine-induced Dsg2 ectodomain cleavage in IECs. Figure 2F shows that the selective ADAM10 inhibitor GI254023X (Hundhausen *et al.*, 2003) dose dependently inhibited the shedding of Dsg2, Dsc2, and E-cadherin ectodomains in the supernatants of TNF-α–treated IECs. GI254023X treatment also inhibited cadherin ectodomain shedding after IL-1β treatment (Supplemental Figure S1E).

Soluble Dsg2 decreases intercellular adhesion in intestinal epithelial cells

Given the role of desmosomes in controlling intercellular adhesion, we evaluated the effect of cadherin extracellular fragments on intestinal epithelial cell–cell adhesion using a dispase assay

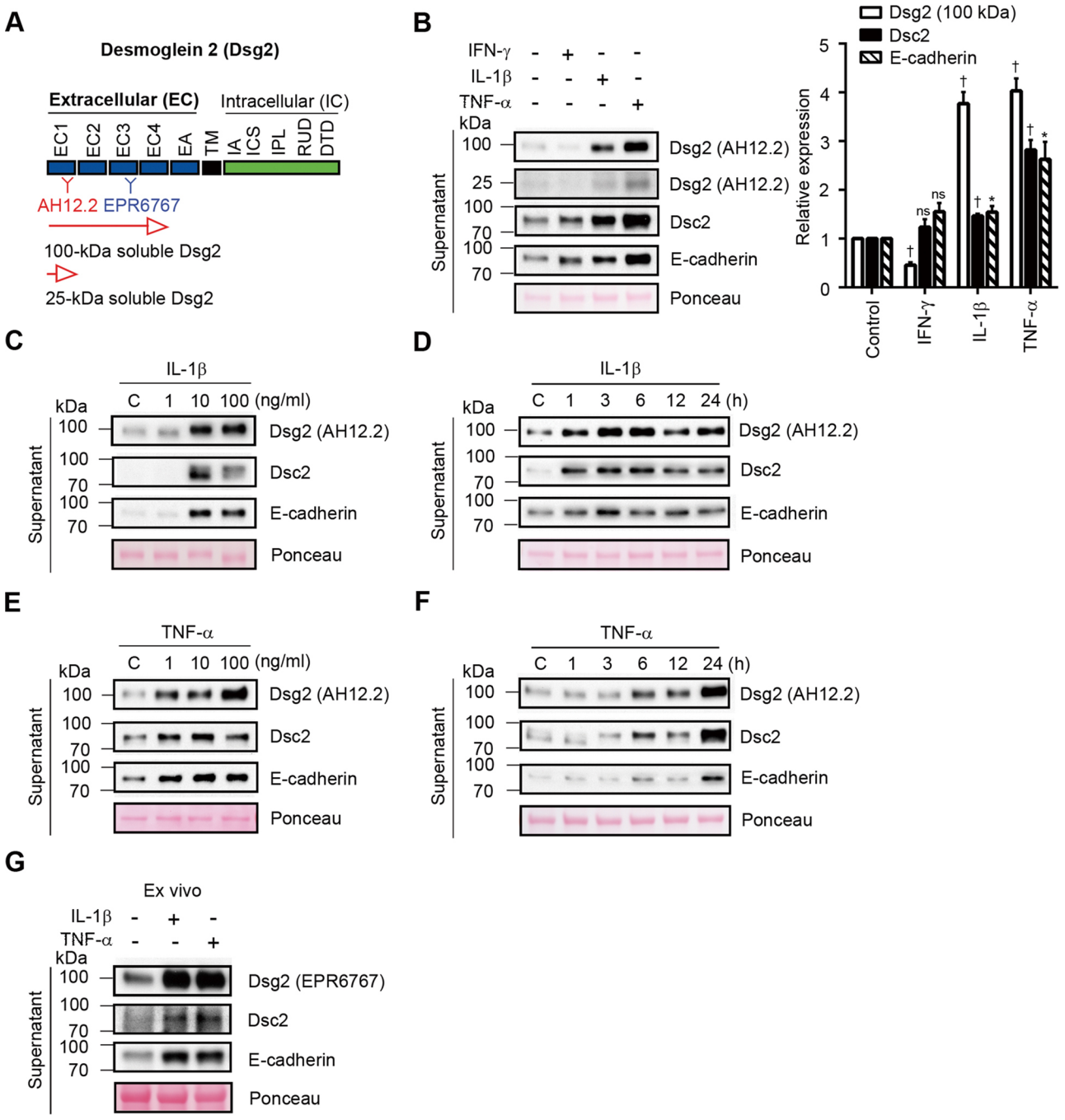

FIGURE 1: Proinflammatory cytokines promote cleavage and shedding of cadherins in intestinal epithelial cells. (A) Schematic representation of protein domain of Dsg2 and epitope mapping of AH12.2 and EPR6767 monoclonal antibodies against Dsg2. EC, extracellular subdomain; EA, extracellular anchor; TM, transmembrane domain; IA, intracellular anchor; ICS, intracellular cadherin-typical sequence; IPL, intracellular proline-rich linker domain; RUD, repeated-unit domain; DTD, desmoglein-specific terminal domain. (B) Immunoblot analysis showing cleavage products of epithelial cadherins in culture supernatants from T84 cells treated with 100 U/ml IFN-γ, 20 ng/ml IL-1β, or 50 ng/ml TNF-α for 24 h. Histograms represent the relative expression of Dsg2 (100 kDa), Dsc2, and E-cadherin cleavage products, as determined by densitometry analysis. Results are expressed as means ± SEM of five independent experiments; $^{*}p < 0.05$, $^{\dagger}p < 0.0001$, ns, not significant, *z* test. (C, D) Immunoblot analysis showing soluble Dsg2 (sDsg2), Dsc2 (sDsc2), and E-cadherin (sE-cadherin) in culture supernatants from T84 cells treated with 1, 10, or 100 ng/ml IL-1β for 6 h (C) or 20 ng/ml IL-1β for up to 24 h (D). (E, F) Immunoblot analysis showing sDsg2, sDsc2, and sE-cadherin in culture supernatants from T84 cells treated with 1, 10, or 100 ng/ml TNF-α for 24 h (E) or 50 ng/ml TNF-α for up to 24 h (F). (G) Immunoblot analysis showing sDsg2, sDsc2, and sE-cadherin in culture supernatants from ex vivo mouse colonic mucosal cultures treated with 20 ng/ml IL-1β or 50 ng/ml TNF-α for 6 h. (B–G) Ponceau staining was used as a loading control. C, control (C–F).

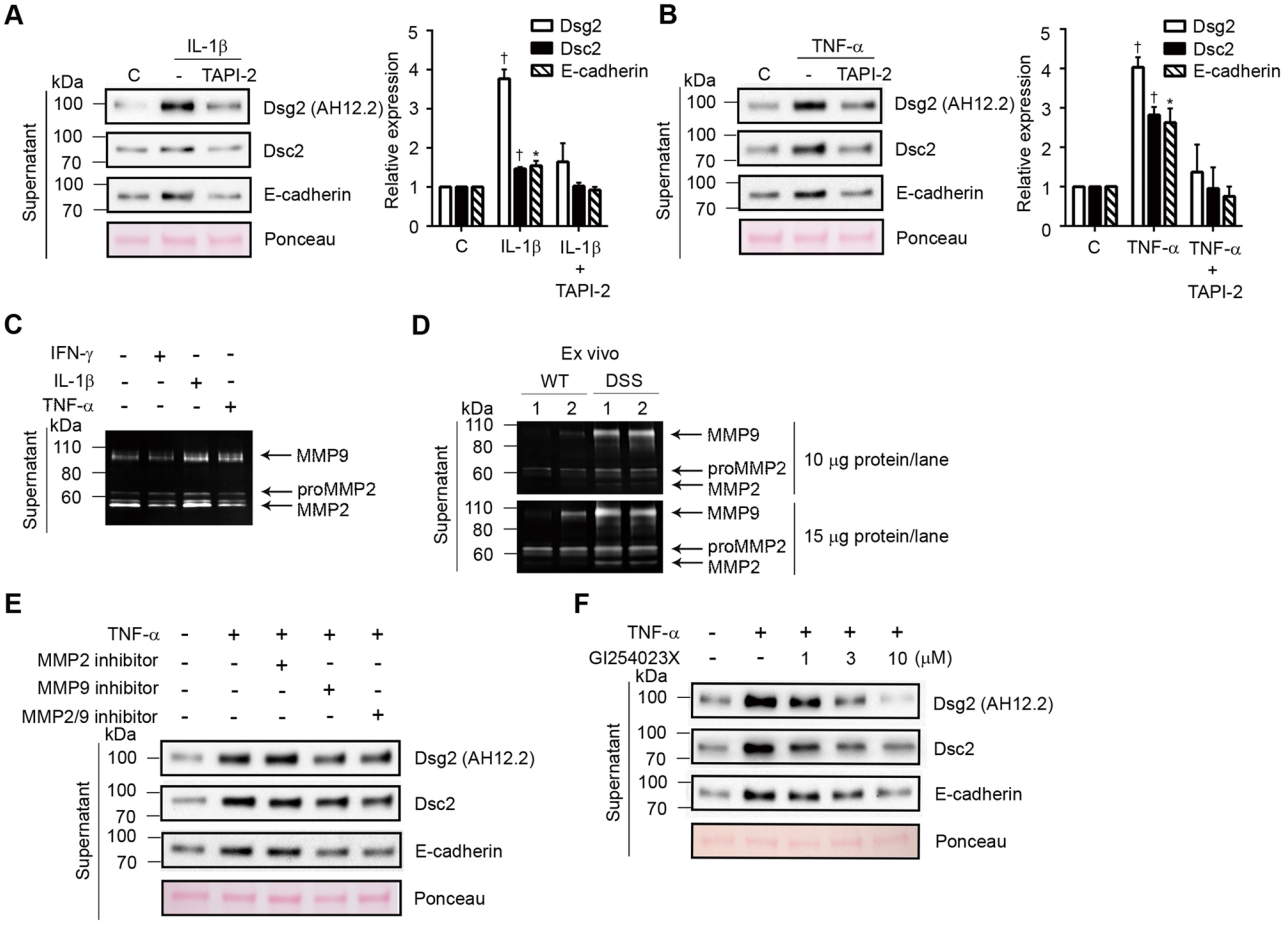

FIGURE 2: MMP9 and ADAM10 cleave cadherin ectodomains in intestinal epithelial cells. (A, B) Immunoblot analysis of soluble Dsg2, Dsc2, and E-cadherin in culture supernatants from T84 cells treated with 20 ng/ml IL-1β for 6 h (A) or 50 ng/ml TNF-α for 24 h (B) in the presence or absence of 20 μM TAPI-2. Histograms represent the relative expression of Dsg2 (100 kDa), Dsc2, and E-cadherin cleavage products, as determined by densitometric analysis. Results are expressed as means ± SEM of five independent experiments; $^{*}p < 0.05$, $^{\dagger}p < 0.0001$, *z* test. (C) Zymographic analysis of MMP2 and 9 activities in culture supernatants from T84 cells treated with 100 U/ml IFN-γ, 20 ng/ml IL-1β, or 50 ng/ml TNF-α for 24 h. (D) Zymographic analysis of MMP2 and 9 activities in the supernatant of ex vivo mouse colonic mucosa cultures derived from wild-type control mice (WT) and mice with DSS-induced colitis (DSS). The colonic mucosa from control and colitic mice was incubated with culture medium for 6 h. The top and bottom images were obtained from gels loaded with a small amount (10 μg/lane) and a large amount (15 μg/lane) of protein in the gels, respectively. (E) Immunoblot analysis of sDsg2, sDsc2, and sE-cadherin in culture supernatants from T84 cells treated with 50 ng/ml TNF-α in the presence or absence of 5 μM MMP2 inhibitor, 100 μM MMP9 inhibitor, or 2.5 μM MMP2/9 inhibitor for 24 h. (F) Immunoblot analysis showing sDsg2, sDsc2, and sE-cadherin in culture supernatants from T84 cells treated with 50 ng/ml TNF-α in the presence or absence of GI254023X (1, 3, or 10 μM) for 24 h. (A, B, E, F) Ponceau staining was used as a loading control. C, control (A, B).

(Klessner *et al.*, 2009; Simpson *et al.*, 2010). A noncontact coculture system was established with T84 IECs cultured in the upper chambers of a Transwell plate and CHO cells stably expressing and secreting sDsg2, sDsc2, or sE-cadherin (Figure 3A) in the lower chambers (Figure 3B). The epithelial monolayers were released from the matrix with dispase and subjected to mechanical stress. The integrity of the epithelial sheet was evaluated as previously described (Klessner *et al.*, 2009; Simpson *et al.*, 2010). As shown in Figure 3C, monolayer fragmentation was increased after coculture with CHO cells secreting Dsg2 EC1–4 domains or E-cadherin EC1–5 domains, but not after coculture with cells secreting Dsc2 EC1–4 domains or Dsg2 EC3+4 domains, compared with control cells. Because *trans* interactions among desmosomal cadherins mediate intercellular adhesion (Chitaev and Troyanovsky, 1997; Syed *et al.*, 2002), we evaluated whether soluble cadherin fragments interfere with these cell–cell associations. We first determined the localization of endogenous cadherins in epithelial cells cocultured with CHO cells secreting cadherin fragments by immunofluorescence labeling and confocal microscopy. Figure 3D shows that the localization of Dsg2, Dsc2, and E-cadherin in the lateral membrane was decreased in epithelial cells exposed to Dsg2 EC1–4 or E-cadherin EC1–5. However, the extent of Dsc2 relocalization from the lateral plasma membrane was not as prominent as observed for Dsg2 and E-cadherin. To determine whether the inhibition of intercellular adhesion mediated by soluble cadherin ectodomain fragments is dependent on interactions with endogenous cadherins, we performed coimmunoprecipitation experiments using T84 IECs exposed to Dsg2 EC1–4 or E-cadherin EC1–5. As shown in Figure 3E, Dsg2 EC1–4 and E-cadherin EC1–5 coimmunoprecipitated with endogenous Dsg2 and E-cadherin. Next we evaluated the association of recombinant ectodomain cadherin

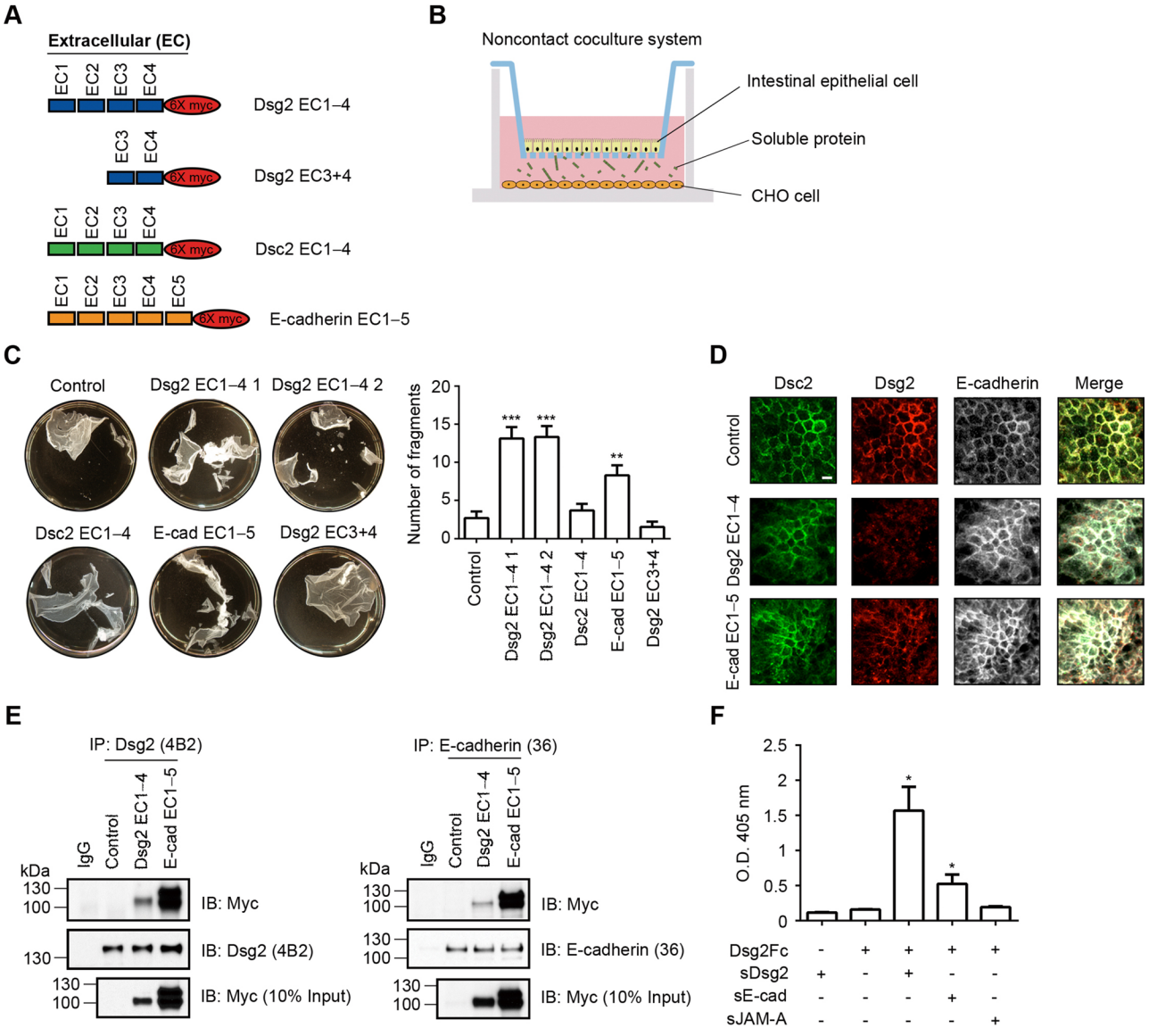

FIGURE 3: Soluble Dsg2 decreases intercellular adhesion of intestinal epithelial cells. (A) Schematic representation of the Dsg2, Dsc2, and E-cadherin ectodomain constructs used in this study. (B) Schematic overview of the noncontact coculture system used in this study. (C) Results of the dispase assay showing the strength of intercellular adhesion in T84 cells cocultured with CHO cells secreting sDsg2, sDsc2, or sE-cadherin for 48 h. Epithelial fragments were quantified as a measure of cell–cell adhesion. Results are expressed as means ± SEM of three independent experiments; $^{**}p < 0.01$, $^{***}p < 0.001$ vs. control, *t* test. (D) Immunofluorescence confocal microscopy (Z-stacks) results show the localization of endogenous Dsc2, Dsg2, and E-cadherin in T84 cells cocultured with CHO cells secreting sDsg2 or sE-cadherin for 48 h. Dsc2, green; Dsg2, red; E-cadherin, white. Scale bar, 10 μm. (E) Coimmunoprecipitation results show the interaction between sDsg2 EC1–4 or sE-cadherin EC1–5 and endogenous Dsg2 or E-cadherin in T84 cells cocultured with CHO cells secreting sDsg2 or sE-cadherin for 24 h. IP, immunoprecipitation; IB, immunoblot. (F) ELISA results showing the binding of sDsg2, sE-cadherin, or soluble JAM-A (sJAM-A, negative control) to immobilized Dsg2Fc. Results are expressed as means ± SEM of three independent experiments; $^{*}p < 0.05$ vs. sDsg2 or Dsg2Fc only, *t* test.

fragments by enzyme-linked immunosorbent assay (ELISA). As shown in Figure 3F, recombinant Fc-tagged Dsg2 (Dsg2Fc) binds to histidine-tagged Dsg2 extracellular fragments (sDsg2-His) purified from the supernatants of CHO cells expressing the Dsg2 ectodomain but does not bind to the extracellular fragments of another epithelial intercellular junction protein, soluble junctional adhesion molecule-A (sJAM-A–His), used as a negative control. Purified sE-cadherin–His also binds to Dsg2Fc but to a lesser extent; this Dsg2 and E-cadherin association was previously reported (Troyanovsky *et al.*, 1999). Together these findings support the homotypic association of sDsg2 and suggest that the binding of sDsg2 and endogenous Dsg2 likely interferes with the *trans* endogenous Dsg2–Dsg2 association between epithelial cells, thereby inhibiting intercellular adhesion and contributing to the relocalization of cell surface cadherin.

Dsg2 extracellular fragments regulate HER2/3-Akt, mTOR, and MAPK signaling pathways and regulate epithelial cell proliferation

Disruption of intercellular adhesion by cleaved junctional proteins has been linked to increased cell proliferation (Lynch *et al.*, 2010).

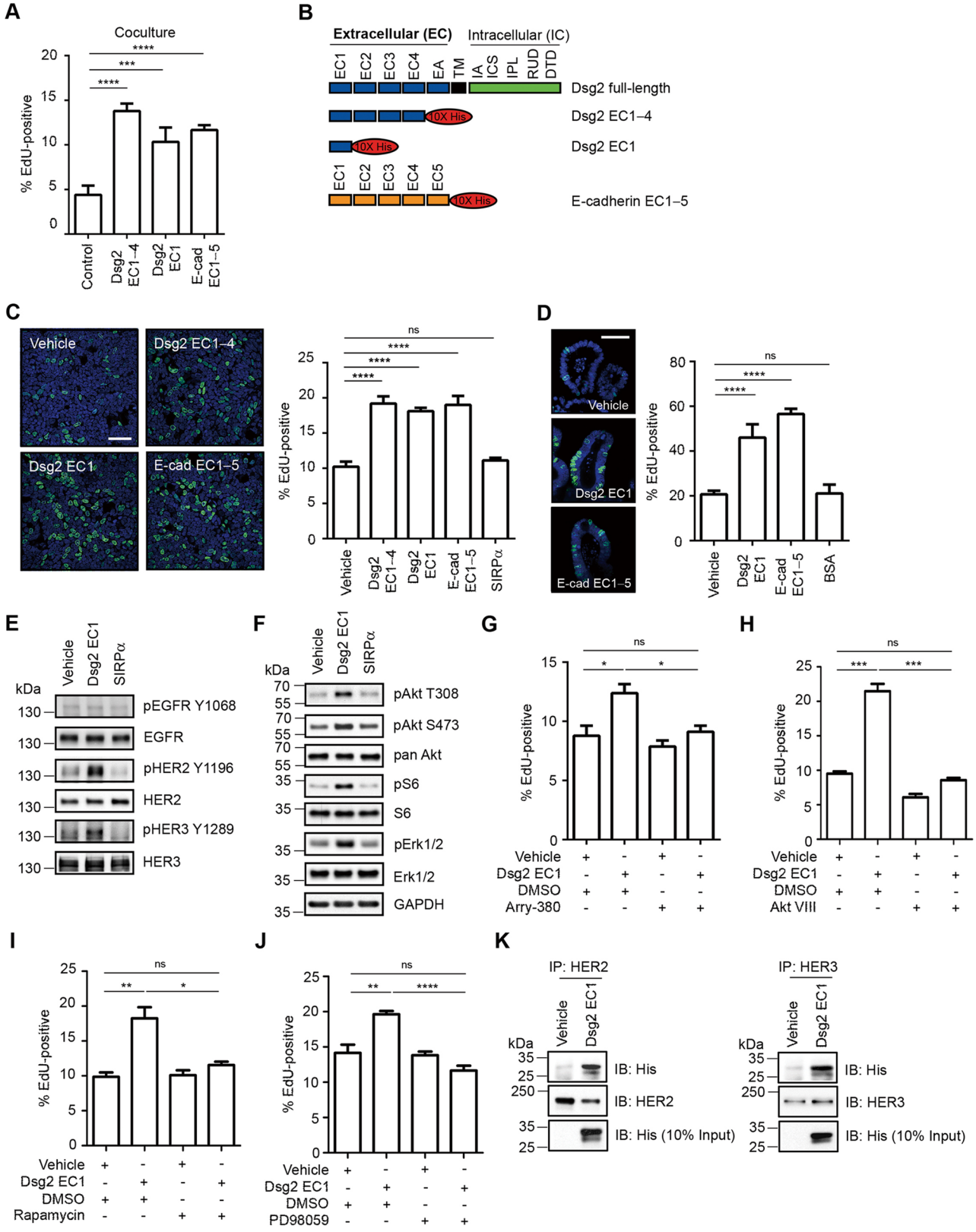

FIGURE 4: Dsg2 extracellular fragments regulate HER2/3-Akt, mTOR, and MAPK signaling pathways and regulate epithelial cell proliferation. (A) T84 cells were cocultured with CHO cells secreting sDsg2 or sE-cadherin, and cell proliferation was evaluated by measuring EdU incorporation into newly synthesized DNA. Images were obtained by confocal microscopy, and EdU-positive nuclei were counted. ***$p < 0.001$, ****$p < 0.0001$ vs. control, *t* test. (B) Schematic representation of Dsg2 and E-cadherin ectodomain constructs used in this study. EC, extracellular subdomain; EA, extracellular anchor; TM, transmembrane domain; IA, intracellular anchor; ICS, intracellular cadherin-typical sequence; IPL, intracellular proline-rich linker domain; RUD, repeated-unit domain; DTD, desmoglein-specific

Therefore we investigated the influence of sDsg2 and sE-cadherin on IEC proliferation using a noncontact coculture system of T84 IECs cocultured with CHO cells secreting Dsg2 EC1–4, Dsg2 EC1, or E-cadherin EC1–5 (Figure 3, A and B). As shown in Figure 4A, the percentage of 5-ethynyl-2′-deoxyuridine (EdU)–positive nuclei in IECs exposed to Dsg2 EC1–4, Dsg2 EC1, or E-cadherin EC1–5 (Figure 4B) was significantly higher than that of IECs cocultured with control CHO cells transfected with an empty expression vector. We sought to confirm these findings by treating IECs with purified Dsg2 EC1–4, Dsg2 EC1, E-cadherin EC1–5, or signal regulatory protein α (SIRPα), an unrelated protein that served as a negative control (Figure 4C). Purified proteins were analyzed by Coomassie staining of gels and immunoblotting (Supplemental Figure S3). Our results showed increased proliferation of IECs exposed to sDsg2 (Dsg2 EC1–4 or Dsg2 EC1) compared with that of IECs exposed to SIRPα, as assessed by EdU incorporation into newly synthesized DNA (Figure 4C). Consistent with results for other cells (Najy *et al.*, 2008; Lynch *et al.*, 2010; Brouxhon *et al.*, 2014a), increased proliferation was also observed for IECs exposed to sE-cadherin (Figure 4C). To verify results obtained using the IEC cell line, we investigated the influence of sDsg2 on proliferation of primary mouse IECs grown as enteroid cultures (Fuller *et al.*, 2012) and observed increased proliferation in cultures exposed to purified Dsg2 EC1 or E-cadherin EC1–5 (Figure 4D). Taken together, the results suggest that Dsg2 EC1 and E-cadherin EC1–5 fragments promote proliferation of IECs.

We next investigated the mechanism by which Dsg2 EC1 promotes IEC proliferation. These analyses focused on sDsg2 because the effects of sE-cadherin have been previously described (Najy *et al.*, 2008; Brouxhon *et al.*, 2014a). Shed ectodomains of epithelial cadherins are believed to promote cell proliferation by activating tyrosine receptor kinases such as human epidermal growth factor receptor (EGFR, also known as HER1; Najy *et al.*, 2008; Klessner *et al.*, 2009; Brouxhon *et al.*, 2014a). We therefore examined EGFR activation in IECs incubated with Dsg2 EC1. Of interest, EGFR phosphorylation was not altered in IECs exposed to either Dsg2 EC1 or SIRPα (negative control; Figure 4E). Therefore we investigated the effect of sDsg2 on the phosphorylation and activation of other HER family members (Citri and Yarden, 2006). Figure 4E shows that exposure to sDsg2, but not to SIRPα, increased phosphorylation of HER2 (Tyr-1196) and HER3 (Tyr-1289), indicating the activation of these receptors; however, HER2 and HER3 protein levels were unchanged after Dsg2 EC1 treatment (Figure 4E). Dimerization and activation of HER2 and HER3 promote tumor growth through MAPK and phosphoinositide 3-kinase/Akt/mTOR signaling (Baselga and Swain, 2009); therefore we investigated whether Dsg2 EC1 can activate these signaling cascades. Indeed, results of densitometric analysis showed increased phosphorylation of Akt Thr-308 (pAkt T308), Akt Ser-473 (pAkt S473), extracellular signal-regulated protein kinase 1/2 Thr-202/Tyr-204 (pErk1/2), and S6 ribosomal protein Ser-235/Ser-236 (pS6) (2.6-, 3.1-, 1.7-, and 2.7-fold increases, respectively) in IECs exposed to sDsg2 EC1; however, total protein levels of Akt, Erk, and S6 in sDsg2-treated IECs did not differ from those of controls (Figure 4F). Exposure to Dsg2 EC1–4 also activated HER2 and HER3 signaling in IECs (Supplemental Figure S4, A and B). To confirm the role of Akt/mTOR and MAPK signaling in mediating sDsg2-induced cellular proliferation, we treated cultures with pharmacologic inhibitors specific for these signaling proteins. As shown in Figure 4, G–J, and Supplemental Figure S4, C–F, inhibition of HER2 (Arry-380), Akt (Akt inhibitor VIII), mTOR complex 1 (mTORC1, rapamycin), and MAPK kinase (MEK, PD98059) inhibited Dsg2 EC1-induced IEC proliferation. Akt inhibition also suppressed proliferation of IECs exposed to Dsg2 EC1–4 (Supplemental Figure S4G). Taken together, these results indicate that sDsg2 activates HER2 and HER3 signaling and IEC proliferation.

Because sE-cadherin fragments have been shown to associate with EGFR, we hypothesized that sDsg2 binds to HER2 or HER3, promoting phosphorylation/activation. Indeed, our results showed that Dsg2 EC1 coimmunoprecipitated with HER2 and HER3 (Figure 4K), and interactions of Dsg2 EC1–4 and sE-cadherin with HER2 and HER3 were observed (Supplemental Figure S4, H and I). In summary, the results suggest that sDsg2 promotes cellular proliferation through activation of HER2 and HER3 and the downstream effectors Akt/mTOR and MAPK.

Increased levels of Dsg2 extracellular fragments in inflamed intestinal mucosa

Increased proinflammatory cytokine and proteinase activities have been reported in the inflamed intestinal mucosa of patients with IBD and in animal models of colitis (Rogler and Andus, 1998; Baugh *et al.*, 1999). For that reason, we investigated Dsg2 cleavage in the intestinal mucosa from patients with active ulcerative colitis that showed neutrophil infiltration and epithelial erosions. Inactive ulcerative colitis (intact epithelium) mucosa was used as a control. As shown in Figure 5A, increased levels of Dsg2 extracellular cleavage fragments (~25 and 50 kDa) were detected in inflamed intestinal mucosa. To confirm cleavage of Dsg2 and E-cadherin in the mucosa during active inflammation, we analyzed colonic mucosa of mice injected with IL-1β or TNF-α. As shown in Figure 5, B and C, cleavage products of Dsg2 and E-cadherin were increased in the mucosa of mice treated with proinflammatory cytokines. Immunoblots detected 100- and 80-kDa fragments corresponding to the ectodomains of Dsg2 and E-cadherin, respectively. Next we confirmed Dsg2 cleavage during inflammation by analyzing the presence of sDsg2 in the mucosa of mice with DSS-induced colitis. DSS

terminal domain. (C) Proliferation of T84 cells treated with sDsg2 (EC1–4 or EC1), sE-cadherin (EC1–5), or SIRPα (negative control) was determined by EdU incorporation. ****$p < 0.0001$ vs. vehicle control; ns, not significant; *t* test. Scale bar, 50 µm. (D) Proliferation of enteroids treated with sDsg2, sE-cadherin, or bovine serum albumin (BSA, negative control) was determined by EdU incorporation. ****$p < 0.0001$ vs. vehicle control; ns, not significant; *t* test. Scale bar, 50 µm. (E) Immunoblot analysis of pEGFR (Y1068), EGFR, pHER2 (Y1196), HER2, pHER3 (Y1289), and HER3 in T84 cells exposed to Dsg2 EC1 or SIRPα (negative control) for 1 h. (F) Immunoblot analysis of EGFR-HER signaling in T84 cells treated with Dsg2 EC1 or SIRPα (negative control) for 1 h. Cell lysates were analyzed by immunoblotting against pAkt (T308, S473), pan Akt, pS6 (S235/S236), S6, pErk1/2 (T202/Y204), and Erk1/2. GAPDH was used as a loading control. (G–J) EdU incorporation showing proliferation of T84 cells treated with Dsg2 EC1 and 100 nM Arry-380 (HER2 inhibitor), 2.12 µM Akt inhibitor VIII, 2 nM rapamycin (mTORC1 inhibitor), or 20 µM PD98059 (MEK inhibitor). *$p < 0.05$, **$p < 0.01$, ***$p < 0.001$, ****$p < 0.0001$; ns, not significant; *t* test. (K) Results of coimmunoprecipitation demonstrating interactions between Dsg2 EC1 and HER2 or HER3 in T84 cells. IP, immunoprecipitation; IB, immunoblotting. (C, D) EdU, green; TO-PRO-3 iodide (nuclei), blue. (A, C, D, G–J) Histograms represent the percentage of nuclei that were EdU-positive. Results are expressed as means ± SEM of at least 10 different fields.

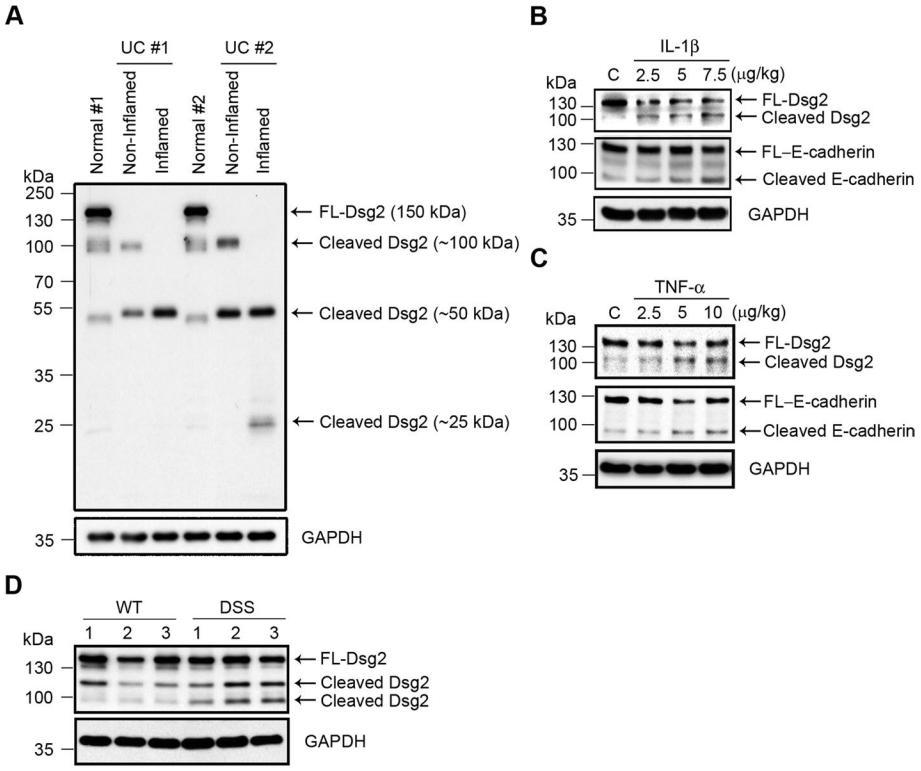

FIGURE 5: Increased levels of Dsg2 extracellular fragments in inflamed intestinal mucosa. (A) Immunoblot analysis of Dsg2 (AH12.2) in noninflamed and inflamed human colonic tissues from patients with ulcerative colitis (UC) and healthy controls (Normal). (B, C) Immunoblot analysis of Dsg2 (EPR6767) and E-cadherin (DECMA-1) in the colonic mucosa of mice that received intraperitoneal injections of IL-1β (B) or TNF-α (C). (D) Immunoblot analysis of Dsg2 protein in the colonic mucosa of mice with DSS-induced colitis (DSS) and wild-type controls (WT). The samples were analyzed using antibodies against Dsg2 clone ERP6767. (A–D) GAPDH was used as a loading control. FL, full-length. C, control (B, C).

treatment was restricted to 4 d to avoid widespread erosions and ulcerations in the colonic mucosa. Figure 5D shows an increase in Dsg2 cleavage (100 kDa) in the mucosa of colitic mice. Taken together, the results indicate that sDsg2 is increased in the colonic mucosa during inflammation.

DISCUSSION

Desmosomes function as spot welds below the adherens junction in simple epithelia, such as intestinal epithelia, to mediate adhesive strength (Tsukita *et al.*, 2008). Our results suggest that proinflammatory cytokines promote ectodomain cleavage of cadherins in columnar IECs by activating the extracellular proteinases MMP9 and ADAM10. Proinflammatory cytokines have been reported to upregulate such extracellular proteinases (Medina and Radomski, 2006; Santana *et al.*, 2006; Pruessmeyer *et al.*, 2010). Both MMP and ADAM proteinases cleave classic cadherins (E-, V-, VE-cadherin), as well as desmosomal cadherin (Dsg2) ectodomains (Lochter *et al.*, 1997; Noe *et al.*, 2001; Maretzky *et al.*, 2005; Bech-Serra *et al.*, 2006; Nava *et al.*, 2013). MMP and ADAM activities are up-regulated not only during inflammation, but also in other pathological conditions, such as cancers, vascular disorders, and autoimmune diseases (Rocks *et al.*, 2008; Gialeli *et al.*, 2011). Cadherin shedding mediated by MMPs and/or ADAMs has been reported in other epithelia, such as the complex skin epithelium, where the shed fragments inhibit intercellular adhesion (Lorch *et al.*, 2004; Maretzky *et al.*, 2005; Reiss *et al.*, 2005; Klessner *et al.*, 2009). In addition, cleavage of the Dsg1 ectodomain in keratinocytes by *Staphylococcus aureus* exfoliative toxin A/B disrupts intercellular adhesion, contributing to the pathogenesis of blistering skin diseases (Amagai *et al.*, 2002). The soluble 80-kDa N-terminal E-cadherin fragment also disrupts adherens junctions (Wheelock *et al.*, 1987; Noe *et al.*, 1999) and has been implicated in the progression of breast, prostate, and skin cancer (Kuefer *et al.*, 2003; Najy *et al.*, 2008; Brouxhon *et al.*, 2014b). Soluble E-cadherin has been detected in the serum of cancer patients, and activation of EGFR and MAPK signaling by sE-cadherin appears to play a role in the growth and survival of the tumors (Wilmanns *et al.*, 2004; Najy *et al.*, 2008; Gogali *et al.*, 2010; Brouxhon *et al.*, 2014a). However, the generation of cadherin fragments and their contribution to epithelial barrier compromise in mucosal inflammatory disorders is not well understood. One of the proposed mechanisms links cadherin ectodomain shedding and decreased intercellular adhesion to the endocytic trafficking of cadherins (Bryant and Stow, 2004), which modifies epithelial adhesion during remodeling in development and cancer cell metastasis (Canel *et al.*, 2013). In this study, we observed that mucosal inflammation also promotes Dsg2 and E-cadherin ectodomain shedding. During inflammation, proinflammatory cytokines induce activation of epithelial-derived MMPs and MMPs from infiltrating neutrophils that can promote cleavage of cadherins, thereby influencing epithelial barrier properties. Analysis of functional effects of cadherin ectodomain fragments on epithelial barrier function revealed decreased transepithelial electrical resistance with corresponding increase in 4-kDa dextran flux in response to sDsg2 and sE-cadherin but not sDsc2 (Supplemental Figure S2, A and B). These results are supported by a previous report that treatment of a Dsg2 antibody directed against extracellular domain disrupts intestinal epithelial barrier function (Schlegel *et al.*, 2010). In this scenario, compromised intercellular adhesion was associated with decreased Dsg2 and E-cadherin in the lateral membrane (Figure 3D). We propose that the shed Dsg2 and E-cadherin ectodomains interfere with *trans* interactions among desmosomal cadherins, which are important for mediating intercellular adhesion (Chitaev and Troyanovsky, 1997; Waschke *et al.*, 2007; Nie *et al.*, 2011). These findings are consistent with the results of studies showing that the soluble N-terminal region of E-cadherin decreases intercellular adhesion (Wheelock *et al.*, 1987; Noe *et al.*, 1999; Symowicz *et al.*, 2007). In this study, we also observed that Dsc2 distribution in the lateral membrane was decreased in epithelial cells exposed to Dsg2 EC1–4 or E-cadherin EC1–5. However, the extent of Dsc2 relocalization from the lateral plasma membrane was not as prominent as observed for Dsg2 and E-cadherin (Figure 3D).

Cadherins mediate bidirectional signaling with receptor tyrosine kinases to control cell behavior (Wheelock and Johnson, 2003). For example, EGFR/HER1 regulates desmosome assembly and function in squamous carcinoma cells by decreasing the cell surface distribution of desmosomal cadherins (Lorch *et al.*, 2004). In

addition, EGFR/HER1, in concert with ADAM17, regulates the shedding and endocytic trafficking of Dsg2 (Klessner *et al.*, 2009). We observed that Dsg2 ectodomains not only inhibit intercellular adhesion, but also increase epithelial cell proliferation. However, we did not observe a change in EGFR/HER1 phosphorylation/activation in response to sDsg2 exposure. The mammalian HER receptor family consists of four closely related growth factor receptors (HER1–4), which mediate cell adhesion, proliferation, and migration (Citri and Yarden, 2006). Our results showing that sDsg2 activates HER2 and HER3 but not EGFR/HER1 are consistent with the results of a study by Najy *et al.* (2008) in breast cancer cells. This unique mechanism is also supported by other reports that proinflammatory cytokines induce the phosphorylation of HER2 in intestinal epithelial cells and that HER2 activation requires ADAM17-dependent shedding of the ligand neuregulin-1 (Finigan *et al.*, 2011; Jijon *et al.*, 2012). On ligand binding, HER receptors dimerize, activating the cytoplasmic kinase domain and initiating downstream signaling (Hynes and lane, 2005). HER2 is the preferred dimerization partner, and HER2-containing heterodimers generate intracellular signals that are stronger than signals emanating from other HER combinations (Pinkas-Kramarski *et al.*, 1996). In this study, we found that sDsg2-induced HER2 and HER3 phosphorylation and downstream activation of Akt/mTOR and MAPK promote IEC proliferation (Figure 4) and HER2–HER3 heterodimerization (Supplemental Figure S4J). Similarly, a previous study demonstrated that ADAM15-mediated E-cadherin cleavage in cancer cells stabilizes HER2 and HER3 heterodimerization and downstream Erk signaling (Najy *et al.*, 2008). We also observed that pharmacological inhibition of Akt and Erk signaling is sufficient to inhibit the hyperproliferative effects of sDsg2. It is known that Akt and/or MAPK activation promote mTORC1 signaling through parallel mechanisms (Winter *et al.*, 2011). Therefore, mTORC1 could be a downstream link between Akt and MAPK signaling and IEC proliferation during inflammation. In addition, IEC proliferation caused by the release of soluble cadherins in the inflamed intestinal mucosa may be mediated by the generation or binding of HER ligands.

A continuous turnover of intercellular junction proteins is observed in healthy individuals and is required for the maintenance of epithelial barriers. Physiologically low levels of cadherin cleavage products have been identified in the serum of healthy individuals. Increased sE-cadherin has been detected in the serum of cancer patients (Wilmanns *et al.*, 2004; Gogali *et al.*, 2010), and their generation likely contributes to tumor biology and metastasis. Our studies suggest that sDsg2 in addition to sE-cadherin are generated in the intestinal mucosa during inflammation. Thus not only does the presence of such cadherin fragments influence epithelial homeostasis, but their detection in the serum could also serve as a biomarker of active inflammation in the mucosa.

Our study provides novel insights into the mechanism by which proinflammatory cytokines released into the epithelial milieu during mucosal inflammation promote cadherin ectodomain shedding, thereby altering homeostasis and barrier function of the intestinal epithelium. Although the compromised epithelial barrier may exacerbate mucosal inflammation, soluble cadherin fragments may also have beneficial effects by promoting the loosening of intercellular contacts and inducing cellular proliferation to stimulate repair of the epithelial barrier (Figure 6).

MATERIALS AND METHODS

Antibodies and reagents

The following primary monoclonal and polyclonal antibodies were used to detect proteins by immunofluorescence microscopy and/or immunoblot analysis: mouse anti-Dsg2 (clone AH12.2, generated in-house; Nava *et al.*, 2007; Kolegraff *et al.*, 2011b), anti-Dsg2 (clone 4B2, a kind gift from K. J. Green, Northwestern University, Evanston, IL), rabbit anti-Dsg2 (clone EPR6767), anti-MMP2 (Novus Biologicals, Littleton, CO), anti-Dsg2 (clone EPR6768), mouse anti-His (clone HIS.H8; Abcam, Cambridge, MA), guinea pig anti-Dsc2 (American Research Products, Waltham, MA), mouse anti-Dsc2/3 (clone 7G6; Life Technologies, Carlsbad, CA), anti–E-cadherin (clone HECD-1, a generous gift from A. S. Yap, University of Queensland, Brisbane St Lucia, Australia; Shimoyama *et al.*, 1989), anti–E-cadherin (clone 36; BD Biosciences, San Jose, CA), rat anti–uvomorulin/E-cadherin (clone DECMA-1), rabbit anti-glyceraldehyde 3-phosphate dehydrogenase (GAPDH), anti-actin (Sigma-Aldrich, St. Louis, MO), mouse anti-JAM-A (clone J10.4, generated in-house; Liu *et al.*, 2000), anti-SIRPα (clone SAF17.2, generated in-house; Lee *et al.*, 2010), anti–Myc-tag (clone 9B11), rabbit anti–phospho-EGFR (Tyr-1068), anti-EGFR, anti–phospho-HER2 (Tyr-1196), anti-HER2, anti–phospho-HER3 (Tyr-1289), anti-HER3, anti–phospho-Akt (Thr-308), anti–phospho-Akt (Ser-473), anti–pan Akt, anti–phospho-S6 ribosomal protein (Ser-235/Ser-236), anti–S6 ribosomal protein, anti–phospho-Erk1/2 (Thr-202/Tyr-204), anti-Erk1/2, and anti-MMP9 (Cell Signaling Technology, Danvers, MA). Fluorophore-conjugated secondary antibodies (Alexa dye series) were obtained from Life Technologies. Horseradish peroxidase (HRP)–conjugated secondary antibodies were obtained from Jackson ImmunoResearch Laboratories (West Grove, PA). Recombinant human IFN-γ, TNF-α, mouse IL-1β, IFN-γ, and TNF-α were purchased from PeproTech (Rocky Hill, NJ). Recombinant human IL-1β was obtained from EMD Millipore (Billerica, MA).

Cell and organ culture

The human T84 intestinal epithelial cell line and CHO cells were cultured as previously described (Ivanov *et al.*, 2007; Kolegraff *et al.*, 2011b). For the noncontact coculture system, T84 cells were seeded on a 3-μm–pore size filter in the inner chamber, and CHO cells were seeded in the outer chamber (Transwell; Corning, Corning, NY). Tissue cultures were prepared from the murine distal colon, which was opened longitudinally and cleaned of fecal contents with cold Hank's balanced salt solution containing 100 U/ml penicillin and 100 μg/ml streptomycin (Life Technologies). The gut was cut into 2-mm^2 pieces and then transferred onto an uncoated 12-well plate (Corning). The tissue pieces were incubated in 1.5 ml RPMI-1640 supplemented with 100 U/ml penicillin and 100 μg/ml streptomycin at 37°C in a 5% CO_2 incubator for 6 h. Culture supernatants were collected for immunoblot analysis or zymography.

Inhibitor treatment

Confluent T84 cells were treated with the following inhibitors 1 h before treatment with sDsg2 (10 μg/ml): 20 μM TAPI-2, 5 μM MMP2 inhibitor IV, 100 μM MMP9 inhibitor II, 2.5 μM MMP2/9 inhibitor II, 2.12 μM Akt inhibitor VIII, 20 μM PD98059 (EMD Millipore), 1–10 μM inhibitor GI254023X (a kind gift from A. Ludwig, RWTH Aachen University, Aachen, Germany; Hundhausen *et al.*, 2003), 100 nM Arry-380 (Selleckchem, Houston, TX), or 2 nM rapamycin (Tocris Bioscience, Bristol, United Kingdom).

Immunoblotting

For in vitro cell cultures, confluent monolayers were collected in lysis buffer (20 mM Tris, 50 mM NaCl, 2 mM EDTA, 2 mM ethylene glycol tetraacetic acid, 1% sodium deoxycholate, 1% Triton X-100, and 0.1% SDS, pH 7.4) containing protease and phosphatase inhibitor cocktails (Sigma-Aldrich). After sonication, the cell lysates

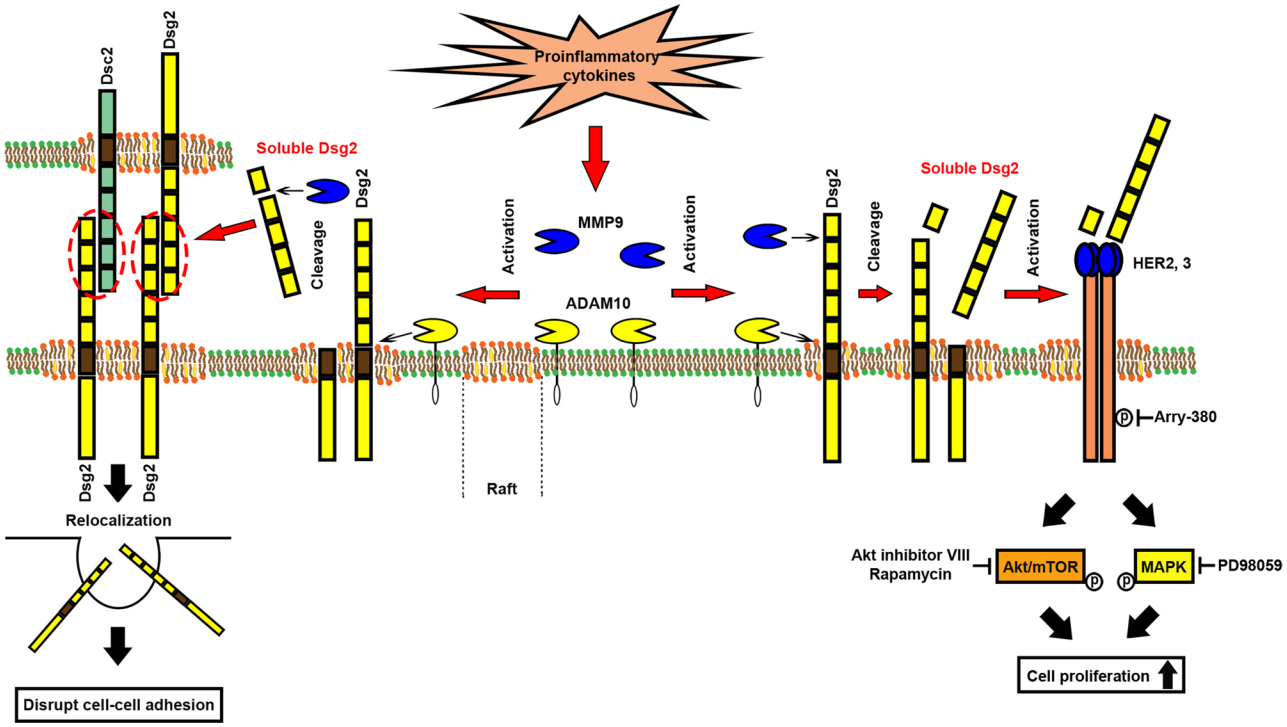

FIGURE 6: Model showing the role of soluble Dsg2 in intestinal epithelial homeostasis. The mechanism by which soluble Dsg2 (sDsg2) mediates intestinal epithelial homeostasis. During inflammation, proinflammatory cytokines IL-1β and TNF-α in the milieu of the epithelium stimulate the activation of proteinases (MMPs and ADAMs) involved in the cleavage of Dsg2 (Figures 1 and 2 and Supplemental Figure S1). sDsg2 interacts with membrane-bound Dsg2 and E-cadherin and induces their relocalization from the plasma membrane, thereby decreasing intercellular adhesion between intestinal epithelial cells (Figure 3). sDsg2 also interacts with HER2 or HER3, activating the Akt/mTOR and MAPK signaling pathways to promote IEC proliferation (Figure 4 and Supplemental Figure S4).

were cleared by centrifugation (5000 × *g* at 4°C for 10 min). For studies with culture supernatants, cells were grown to confluency and switched to serum-free medium 24 h before sample collection. The supernatants were cleared by centrifugation to remove cell debris and concentrated 10-fold using Amicon Ultra Centrifugal Filters (3K MW; EMD Millipore). For analysis with human and mouse colonic mucosa specimens, the samples were resuspended in lysis buffer, homogenized, and sonicated as described. Protein concentration was determined using a Pierce BCA Protein Assay Kit (Thermo Fisher Scientific, Marietta, OH). The samples were then resuspended in NuPAGE LDS Sample Buffer (Life Technologies) and loaded onto polyacrylamide gels (15–20 µg protein/lane). After electrophoresis, the separated protein bands were transferred to a polyvinylidene fluoride membrane (Bio-Rad, Hercules, CA) and probed with primary antibodies. Secondary antibodies conjugated to HRP were used to visualize the protein bands. Staining with Ponceau S solution (Sigma-Aldrich) was used to show equal loading of proteins. Immunoblots were quantified using ImageJ (National Institutes of Health, Bethesda, MD).

Zymography

Culture supernatants were concentrated using an Amicon Ultra Centrifugal Filter (3K MW) according to the manufacturer's instructions and loaded on a Novex 10% Zymogram Gel containing 0.1% (wt/vol) gelatin (Life Technologies). After electrophoresis, the gels were washed twice in renaturing buffer (Life Technologies) and then incubated at 37°C for 24 h in developing buffer (Life Technologies). To visualize proteinase activity, the gels were stained with SimplyBlue SafeStain (Life Technologies).

Generation of stable cell lines

CHO cells were transfected with the empty neomycin-resistant pcDNA3.1 expression vector (Life Technologies) as a control or pcDNA3.1 vectors expressing soluble Dsg2 EC1–4, Dsg2 EC3+4, Dsg2 EC1, Dsc2 EC1–4, or E-cadherin EC1–5 (generated by the Emory Cloning Core Facility, Atlanta, GA) and grown in the presence of G418 Sulfate (Mediatech, Manassas, VA) to select transfected cells. Monoclonal cell populations were isolated by the limiting dilution method.

Dispase assay

Cell monolayers were treated with 2.4 U/ml Dispase II (Roche Diagnostics, Mannheim, Germany) in phosphate-buffered saline (PBS) with calcium and magnesium at 37°C for 30 min. The cells were then transferred to 15-ml conical tubes containing 5 ml of PBS, which were gently mixed by rotating in a tube rotator 10–30 times. Monolayer fragments were transferred to 12-well tissue culture plates (Corning), imaged using a dissecting microscope, and counted.

Immunofluorescence microscopy

Cells grown on filters were fixed and permeabilized with ice-cold absolute methanol at –20°C for 20 min or 4% paraformaldehyde

at room temperature for 10 min, followed by treatment with 0.5% Triton X-100 at room temperature for 5 min. Nonspecific protein binding was blocked by 3% bovine serum albumin (Sigma-Aldrich) in PBS at z for 1 h, and the cells were incubated with primary antibodies at 4°C overnight, washed in PBS, and subsequently labeled with secondary antibodies at room temperature for 1 h. Nuclei were stained using TO-PRO-3 iodide (Life Technologies) in PBS at room temperature for 15 min. Samples were mounted using VECTASHIELD (Vector Laboratories, Burlingame, CA) and visualized on a Zeiss LSM 510 Meta Confocal microscope (Carl Zeiss Microimaging, Thornwood, NY).

Immunoprecipitation

Confluent T84 cell monolayers were homogenized and lysed in lysis buffer containing 100 mM KCl, 10 mM NaCl, 3.5 mM $MgCl_2$, 10 mM 4-(2-hydroxyethyl)-1-piperazineethanesulfonic acid (HEPES) (pH 7.4), 1% Nonidet P-40, and protease and phosphatase inhibitor cocktails. The lysates were cleared by centrifugation (4000 rpm at 4°C for 4 min) and then incubated overnight with mouse anti-Dsg2 (clone 4B2), anti–E-cadherin (clone 36), or isotype-matched control immunoglobulin G (IgG; Sigma-Aldrich) or incubated overnight with rabbit anti-HER2, anti-HER3, or isotype-matched control IgG. After addition of Protein A/G Sepharose Fast Flow (GE Healthcare, Little Chalfont, United Kingdom), the supernatants were incubated at 4°C for 3 h. The immunocomplexes were washed four times, boiled in NuPAGE LDS Sample Buffer, and then separated by SDS–PAGE for protein analysis.

Recombinant proteins

The Dsg2 extracellular domain, E-cadherin, JAM-A, and SIRPα were cloned into pcDNA3.0 with a His tag and transfected into CHO or HEK293T cells with 25 µg/ml polyethylenimine. The cell supernatants were collected, and the His-tagged proteins were purified using nickel beads (Thermo Fisher Scientific). Purified proteins were analyzed by Coomassie staining (Imperial Protein Stain; Thermo Fisher Scientific) of gels and immunoblotting (Supplemental Figure S3).

ELISA

Immulon 2 HB plates (Thermo Fisher Scientific) were coated with 5 µg of recombinant human Dsg2 Fc (R&D Systems, Minneapolis, MN) and incubated with casein (Roche Diagnostics) to block nonspecific protein binding and with 0.5 µg/ml sDsg2-His, sE-cadherin-His, or sJAM-A-His in PBS for 1 h. The binding of Dsg2, E-cadherin, and JAM-A was detected using mouse anti-His antibody and goat anti-mouse HRP-conjugated antibody.

Enteroid culture

Intestinal crypts were isolated and cultured as described previously (Mahe *et al.*, 2013) with modifications. Briefly, sections of the small intestine (~10 cm) from 8-wk-old C57BL/6 mice were dissected and opened longitudinally. The sections were cut into 1-cm pieces, washed three times with cold PBS, and incubated with 5 ml of chelation buffer (2 mM EDTA in PBS) at 4°C for 30 min on a rotating wheel. The chelation buffer was changed to 5 ml of cell dissociation buffer (PBS containing 43.3 mM sucrose and 54.9 mM sorbitol), and the epithelium was detached by vigorous shaking. The suspension was passed through a 70-mm cell strainer (BD Biosciences) to remove villi. The resulting crypt suspension was diluted with dissociation buffer, bringing the volume to 10 ml, and the detached crypts were counted in 20-µl droplets. The desired number of crypts was centrifuged at 150 × *g* for 10 min at 4°C in 10 ml of dissociation buffer. The pelleted crypts were resuspended in Matrigel (BD Biosciences) containing 50 ng/ml epidermal growth factor (EGF), 100 ng/ml Noggin, and 500 ng/ml R-spondin (R&D Systems) at 500 crypts/50 µl Matrigel, seeded in the middle of 24-well cell culture plate wells (Corning), and incubated for 30 min at 37°C. The gels were overlaid with 450 µl of minigut culture medium consisting of Advanced DMEM/F12, L-glutamine (2 mM), penicillin (100 U/ml)/streptomycin (100 µg/ml), HEPES (10 mM), B27 supplement (1:50; Life Technologies), and N2 supplement (1:100; R&D Systems). The minigut medium supplemented with EGF, Noggin, and R-spondin was replaced every 4 d, and the enteroids were passaged into fresh Matrigel every 8 d. Enteroids were cultured at 37°C in a 5% CO_2 atmosphere for at least 3 d before stimulation with sDsg2 or sE-cadherin.

EdU incorporation assay

Cells and intestinal crypt organoids were pulse-labeled with EdU (10 nM; Click-iT EdU; Life Technologies) for 1 h and processed according to the manufacturer's instructions.

Human colon samples

Human ulcerative colitis and normal colonic tissue specimens were obtained from the Human Tissue Procurement Service at Emory University. All procedures were approved by the Institutional Review Board at Emory University.

In vivo experiments

Female C57Bl/6J mice (6–8 wk old) were purchased from Jackson Laboratory (Bar Harbor, ME). Mice were intraperitoneally injected with recombinant mouse IL-1β (2.5, 5, or 7.5 µg/kg) or recombinant mouse TNF-α (2.5, 5, or 10 µg/kg) as previously described (Nava *et al.*, 2014). To generate a mouse model of colitis, the mice were treated with DSS (2.5% [wt/vol]; molecular mass, 36–50 kDa; MP Biomedicals, Santa Ana, CA) for 7 d, as previously described (Cooper *et al.*, 1993). All animal protocols were approved by the Institutional Animal Care and Use Committee of Emory University.

Measurement of transepithelial electrical resistance

Cells were cultured on Transwell inserts with 3-µm–pore size filters (Corning). Transepithelial electrical resistance was measured using an EVOM voltmeter with an ENDOHM-12 (World Precision Instruments, Sarasota, FL). Electrical resistance was expressed as $\Omega \times cm^2$. For calculation, the resistance of blank filters was subtracted from that of filters covered with cells.

Measurement of paracellular permeability

To determine the paracellular flux, cells were cultured on Transwell filters with 3-µm pore size (Corning). A 4-kDa fluorescein isothiocyanate–dextran (FD4; Sigma-Aldrich)–containing medium was added to the inner chamber. Samples were collected from the outer chamber at 30, 60, 90, and 120 min. Permeability across cell monolayers was assessed for fluorescence in a microplate fluorescence reader (FL-500; BioTek, Winooski, VT) at an excitation wavelength of 485 nm and an emission wavelength of 530 nm and was expressed as $\mu g/h/cm^2$.

Statistics

For control-normalized experiments, group means were compared by the *z* test. Unpaired Student's *t* test was used to analyze data from all other experiments. Results are displayed as means ± SEM; $p < 0.05$ was considered significant.

ACKNOWLEDGMENTS

We thank our colleagues Ross Hamilton, C. Robert Rankin, Anna Lukacher, and Ingrid McCall for their technical help and discussions. This work was supported by the 12th GlaxoSmithKline International Award from the Japan Society of Immunology and Allergology in Otolaryngology (R.K.), an American Gastroenterological Association Research Scholar Award (P.N.), a Crohn's and Colitis Foundation of America Career Development Award (P.N.), CONACyT Grant 175854 (P.N.), and National Institutes of Health Grants DK061379 (C.A.P.) and DK055679 and DK059888 (A.N.).

REFERENCES

Allen E, Yu QC, Fuchs E (1996). Mice expressing a mutant desmosomal cadherin exhibit abnormalities in desmosomes, proliferation, and epidermal differentiation. J Cell Biol 133, 1367–1382.

Amagai M, Yamaguchi T, Hanakawa Y, Nishifuji K, Sugai M, Stanley JR (2002). Staphylococcal exfoliative toxin B specifically cleaves desmoglein 1. J Invest Dermatol 118, 845–850.

Baselga J, Swain SM (2009). Novel anticancer targets: revisiting ERBB2 and discovering ERBB3. Nat Rev Cancer 9, 463–475.

Baugh MD, Perry MJ, Hollander AP, Davies DR, Cross SS, Lobo AJ, Taylor CJ, Evans GS (1999). Matrix metalloproteinase levels are elevated in inflammatory bowel disease. Gastroenterology 117, 814–822.

Bech-Serra JJ, Santiago-Josefat B, Esselens C, Saftig P, Baselga J, Arribas J, Canals F (2006). Proteomic identification of desmoglein 2 and activated leukocyte cell adhesion molecule as substrates of ADAM17 and ADAM10 by difference gel electrophoresis. Mol Cell Biol 26, 5086–5095.

Brennan D, Hu Y, Joubeh S, Choi YW, Whitaker-Menezes D, O'Brien T, Uitto J, Rodeck U, Mahoney MG (2007). Suprabasal Dsg2 expression in transgenic mouse skin confers a hyperproliferative and apoptosis-resistant phenotype to keratinocytes. J Cell Sci 120, 758–771.

Brouxhon SM, Kyrkanides S, Teng X, Athar M, Ghazizadeh S, Simon M, O'Banion MK, Ma L (2014a). Soluble E-cadherin: a critical oncogene modulating receptor tyrosine kinases, MAPK and PI3K/Akt/mTOR signaling. Oncogene 33, 225–235.

Brouxhon SM, Kyrkanides S, Teng X, O'Banion MK, Clarke R, Byers S, Ma L (2014b). Soluble-E-cadherin activates HER and IAP family members in HER2+ and TNBC human breast cancers. Mol Carcinog 53, 893–906.

Bruewer M, Luegering A, Kucharzik T, Parkos CA, Madara JL, Hopkins AM, Nusrat A (2003). Proinflammatory cytokines disrupt epithelial barrier function by apoptosis-independent mechanisms. J Immunol 171, 6164–6172.

Bryant DM, Stow JL (2004). The ins and outs of E-cadherin trafficking. Trends Cell Biol 14, 427–434.

Canel M, Serrels A, Frame MC, Brunton VG (2013). E-cadherin-integrin crosstalk in cancer invasion and metastasis. J Cell Sci 126, 393–401.

Chitaev NA, Troyanovsky SM (1997). Direct Ca^{2+}-dependent heterophilic interaction between desmosomal cadherins, desmoglein and desmocollin, contributes to cell-cell adhesion. J Cell Biol 138, 193–201.

Citri A, Yarden Y (2006). EGF-ERBB signalling: towards the systems level. Nat Rev Mol Cell Biol 7, 505–516.

Cooper HS, Murthy SN, Shah RS, Sedergran DJ (1993). Clinicopathologic study of dextran sulfate sodium experimental murine colitis. Lab Invest 69, 238–249.

David JM, Rajasekaran AK (2012). Dishonorable discharge: the oncogenic roles of cleaved E-cadherin fragments. Cancer Res 72, 2917–2923.

Dusek RL, Attardi LD (2011). Desmosomes: new perpetrators in tumour suppression. Nat Rev Cancer 11, 317–323.

Dusek RL, Getsios S, Chen F, Park JK, Amargo EV, Cryns VL, Green KJ (2006). The differentiation-dependent desmosomal cadherin desmoglein 1 is a novel caspase-3 target that regulates apoptosis in keratinocytes. J Biol Chem 281, 3614–3624.

Finigan JH, Faress JA, Wilkinson E, Mishra RS, Nethery DE, Wyler D, Shatat M, Ware LB, Matthay MA, Mason R, *et al.* (2011). Neuregulin-1-human epidermal receptor-2 signaling is a central regulator of pulmonary epithelial permeability and acute lung injury. J Biol Chem 286, 10660–10670.

Fuller MK, Faulk DM, Sundaram N, Shroyer NF, Henning SJ, Helmrath MA (2012). Intestinal crypts reproducibly expand in culture. J Surg Res 178, 48–54.

Getsios S, Amargo EV, Dusek RL, Ishii K, Sheu L, Godsel LM, Green KJ (2004). Coordinated expression of desmoglein 1 and desmocollin 1 regulates intercellular adhesion. Differentiation 72, 419–433.

Getsios S, Simpson CL, Kojima S, Harmon R, Sheu LJ, Dusek RL, Cornwell M, Green KJ (2009). Desmoglein 1-dependent suppression of EGFR signaling promotes epidermal differentiation and morphogenesis. J Cell Biol 185, 1243–1258.

Gialeli C, Theocharis AD, Karamanos NK (2011). Roles of matrix metalloproteinases in cancer progression and their pharmacological targeting. FEBS J 278, 16–27.

Gogali A, Charalabopoulos K, Zampira I, Konstantinidis AK, Tachmazoglou F, Daskalopoulos G, Constantopoulos SH, Dalavanga Y (2010). Soluble adhesion molecules E-cadherin, intercellular adhesion molecule-1, and E-selectin as lung cancer biomarkers. Chest 138, 1173–1179.

Green KJ, Simpson CL (2007). Desmosomes: new perspectives on a classic. J Invest Dermatol 127, 2499–2515.

Holthofer B, Windoffer R, Troyanovsky S, Leube RE (2007). Structure and function of desmosomes. Int Rev Cytol 264, 65–163.

Hundhausen C, Misztela D, Berkhout TA, Broadway N, Saftig P, Reiss K, Hartmann D, Fahrenholz F, Postina R, Matthews V, *et al.* (2003). The disintegrin-like metalloproteinase ADAM10 is involved in constitutive cleavage of CX3CL1 (fractalkine) and regulates CX3CL1-mediated cell-cell adhesion. Blood 102, 1186–1195.

Hynes NE, Lane HA (2005). ERBB receptors and cancer: the complexity of targeted inhibitors. Nat Rev Cancer 5, 341–354.

Ivanov AI, Bachar M, Babbin BA, Adelstein RS, Nusrat A, Parkos CA (2007). A unique role for nonmuscle myosin heavy chain IIA in regulation of epithelial apical junctions. PLoS One 2, e658.

Jijon HB, Buret A, Hirota CL, Hollenberg MD, Beck PL (2012). The EGF receptor and HER2 participate in TNF-α-dependent MAPK activation and IL-8 secretion in intestinal epithelial cells. Mediators Inflamm 2012, 207398.

Kamekura R, Kolegraff KN, Nava P, Hilgarth RS, Feng M, Parkos CA, Nusrat A (2014). Loss of the desmosomal cadherin desmoglein-2 suppresses colon cancer cell proliferation through EGFR signaling. Oncogene 33, 4531–4536.

Klessner JL, Desai BV, Amargo EV, Getsios S, Green KJ (2009). EGFR and ADAMs cooperate to regulate shedding and endocytic trafficking of the desmosomal cadherin desmoglein 2. Mol Biol Cell 20, 328–337.

Koch S, Nusrat A (2012). The life and death of epithelia during inflammation: lessons learned from the gut. Annu Rev Pathol 7, 35–60.

Kolegraff K, Nava P, Helms MN, Parkos CA, Nusrat A (2011a). Loss of desmocollin-2 confers a tumorigenic phenotype to colonic epithelial cells through activation of Akt/β-catenin signaling. Mol Biol Cell 22, 1121–1134.

Kolegraff K, Nava P, Laur O, Parkos CA, Nusrat A (2011b). Characterization of full-length and proteolytic cleavage fragments of desmoglein-2 in native human colon and colonic epithelial cell lines. Cell Adh Migr 5, 306–314.

Kuefer R, Hofer MD, Gschwend JE, Pienta KJ, Sanda MG, Chinnaiyan AM, Rubin MA, Day ML (2003). The role of an 80 kDa fragment of E-cadherin in the metastatic progression of prostate cancer. Clin Cancer Res 9, 6447–6452.

Lee WY, Weber DA, Laur O, Stowell SR, McCall I, Andargachew R, Cummings RD, Parkos CA (2010). The role of *cis* dimerization of signal regulatory protein α (SIRPα) in binding to CD47. J Biol Chem 285, 37953–37963.

Liu Y, Nusrat A, Schnell FJ, Reaves TA, Walsh S, Pochet M, Parkos CA (2000). Human junction adhesion molecule regulates tight junction resealing in epithelia. J Cell Sci 113, 2363–2374.

Lochter A, Galosy S, Muschler J, Freedman N, Werb Z, Bissell MJ (1997). Matrix metalloproteinase stromelysin-1 triggers a cascade of molecular alterations that leads to stable epithelial-to-mesenchymal conversion and a premalignant phenotype in mammary epithelial cells. J Cell Biol 139, 1861–1872.

Lorch JH, Klessner J, Park JK, Getsios S, Wu YL, Stack MS, Green KJ (2004). Epidermal growth factor receptor inhibition promotes desmosome assembly and strengthens intercellular adhesion in squamous cell carcinoma cells. J Biol Chem 279, 37191–37200.

Lynch CC, Vargo-Gogola T, Matrisian LM, Fingleton B (2010). Cleavage of E-cadherin by matrix metalloproteinase-7 promotes cellular proliferation in nontransformed cell lines via activation of RhoA. J Oncol 2010, 530745.

Mahe MM, Aihara E, Schumacher MA, Zavros Y, Montrose MH, Helmrath MA, Sato T, Shroyer NF (2013). Establishment of gastrointestinal epithelial organoids. Curr Protoc Mouse Biol 3, 217–240.

Marchiando AM, Graham WV, Turner JR (2010). Epithelial barriers in homeostasis and disease. Annu Rev Pathol 5, 119–144.

Maretzky T, Reiss K, Ludwig A, Buchholz J, Scholz F, Proksch E, de Strooper B, Hartmann D, Saftig P (2005). ADAM10 mediates E-cadherin shedding

and regulates epithelial cell-cell adhesion, migration, and β-catenin translocation. Proc Natl Acad Sci USA 102, 9182–9187.
Maretzky T, Scholz F, Koten B, Proksch E, Saftig P, Reiss K (2008). ADAM10-mediated E-cadherin release is regulated by proinflammatory cytokines and modulates keratinocyte cohesion in eczematous dermatitis. J Invest Dermatol 128, 1737–1746.
Medina C, Radomski MW (2006). Role of matrix metalloproteinases in intestinal inflammation. J Pharmacol Exp Ther 318, 933–938.
Medina C, Videla S, Radomski A, Radomski MW, Antolin M, Guarner F, Vilaseca J, Salas A, Malagelada JR (2003). Increased activity and expression of matrix metalloproteinase-9 in a rat model of distal colitis. Am J Physiol Gastrointest Liver Physiol 284, G116–G122.
Najy AJ, Day KC, Day ML (2008). The ectodomain shedding of E-cadherin by ADAM15 supports ErbB receptor activation. J Biol Chem 283, 18393–18401.
Nava P, Kamekura R, Nusrat A (2013). Cleavage of transmembrane junction proteins and their role in regulating epithelial homeostasis. Tissue Barriers 1, e24783.
Nava P, Kamekura R, Quiros M, Medina-Contreras O, Hamilton RW, Kolegraff KN, Koch S, Candelario A, Romo-Parra H, Laur O, *et al.* (2014). IFNγ-induced suppression of β-catenin signaling: Evidence for roles of Akt and 14.3.3ζ. Mol Biol Cell 25, 2894–2904.
Nava P, Koch S, Laukoetter MG, Lee WY, Kolegraff K, Capaldo CT, Beeman N, Addis C, Gerner-Smidt K, Neumaier I, *et al.* (2010). Interferon-γ regulates intestinal epithelial homeostasis through converging β-catenin signaling pathways. Immunity 32, 392–402.
Nava P, Laukoetter MG, Hopkins AM, Laur O, Gerner-Smidt K, Green KJ, Parkos CA, Nusrat A (2007). Desmoglein-2: a novel regulator of apoptosis in the intestinal epithelium. Mol Biol Cell 18, 4565–4578.
Nie Z, Merritt A, Rouhi-Parkouhi M, Tabernero L, Garrod D (2011). Membrane-impermeable cross-linking provides evidence for homophilic, isoform-specific binding of desmosomal cadherins in epithelial cells. J Biol Chem 286, 2143–2154.
Noe V, Fingleton B, Jacobs K, Crawford HC, Vermeulen S, Steelant W, Bruyneel E, Matrisian LM, Mareel M (2001). Release of an invasion promoter E-cadherin fragment by matrilysin and stromelysin-1. J Cell Sci 114, 111–118.
Noe V, Willems J, Vandekerckhove J, Roy FV, Bruyneel E, Mareel M (1999). Inhibition of adhesion and induction of epithelial cell invasion by HAV-containing E-cadherin-specific peptides. J Cell Sci 112, 127–135.
Pinkas-Kramarski R, Soussan L, Waterman H, Levkowitz G, Alroy I, Klapper L, Lavi S, Seger R, Ratzkin BJ, Sela M, *et al.* (1996). Diversification of Neu differentiation factor and epidermal growth factor signaling by combinatorial receptor interactions. EMBO J 15, 2452–2467.
Pruessmeyer J, Martin C, Hess FM, Schwarz N, Schmidt S, Kogel T, Hoettecke N, Schmidt B, Sechi A, Uhlig S, *et al.* (2010). A disintegrin and metalloproteinase 17 (ADAM17) mediates inflammation-induced shedding of syndecan-1 and -4 by lung epithelial cells. J Biol Chem 285, 555–564.
Reiss K, Maretzky T, Ludwig A, Tousseyn T, de Strooper B, Hartmann D, Saftig P (2005). ADAM10 cleavage of N-cadherin and regulation of cell-cell adhesion and β-catenin nuclear signalling. EMBO J 24, 742–752.
Rocks N, Paulissen G, El Hour M, Quesada F, Crahay C, Gueders M, Foidart JM, Noel A, Cataldo D (2008). Emerging roles of ADAM and ADAMTS metalloproteinases in cancer. Biochimie 90, 369–379.
Rogler G, Andus T (1998). Cytokines in inflammatory bowel disease. World J Surg 22, 382–389.
Santana A, Medina C, Paz-Cabrera MC, Diaz-Gonzalez F, Farre E, Salas A, Radomski MW, Quintero E (2006). Attenuation of dextran sodium sulphate induced colitis in matrix metalloproteinase-9 deficient mice. World J Gastroenterol 12, 6464–6472.
Schlegel N, Meir M, Heupel WM, Holthofer B, Leube RE, Waschke J (2010). Desmoglein 2-mediated adhesion is required for intestinal epithelial barrier integrity. Am J Physiol Gastrointest Liver Physiol 298, G774–G783.
Sewpaul A, French JJ, Khoo TK, Kernohan M, Kirby JA, Charnley RM (2009). Soluble E-cadherin: an early marker of severity in acute pancreatitis. HPB Surg 2009, 397375.
Shimoyama Y, Hirohashi S, Hirano S, Noguchi M, Shimosato Y, Takeichi M, Abe O (1989). Cadherin cell-adhesion molecules in human epithelial tissues and carcinomas. Cancer Res 49, 2128–2133.
Simpson CL, Kojima S, Cooper-Whitehair V, Getsios S, Green KJ (2010). Plakoglobin rescues adhesive defects induced by ectodomain truncation of the desmosomal cadherin desmoglein 1: implications for exfoliative toxin-mediated skin blistering. Am J Pathol 177, 2921–2937.
Steck N, Hoffmann M, Sava IG, Kim SC, Hahne H, Tonkonogy SL, Mair K, Krueger D, Pruteanu M, Shanahan F, *et al.* (2011). Enterococcus faecalis metalloprotease compromises epithelial barrier and contributes to intestinal inflammation. Gastroenterology 141, 959–971.
Syed SE, Trinnaman B, Martin S, Major S, Hutchinson J, Magee AI (2002). Molecular interactions between desmosomal cadherins. Biochem J 362, 317–327.
Symowicz J, Adley BP, Gleason KJ, Johnson JJ, Ghosh S, Fishman DA, Hudson LG, Stack MS (2007). Engagement of collagen-binding integrins promotes matrix metalloproteinase-9-dependent E-cadherin ectodomain shedding in ovarian carcinoma cells. Cancer Res 67, 2030–2039.
Troyanovsky RB, Klingelhofer J, Troyanovsky S (1999). Removal of calcium ions triggers a novel type of intercadherin interaction. J Cell Sci 112, 4379–4387.
Tselepis C, Chidgey M, North A, Garrod D (1998). Desmosomal adhesion inhibits invasive behavior. Proc Natl Acad Sci USA 95, 8064–8069.
Tsukita S, Yamazaki Y, Katsuno T, Tamura A, Tsukita S (2008). Tight junction-based epithelial microenvironment and cell proliferation. Oncogene 27, 6930–6938.
Waschke J, Menendez-Castro C, Bruggeman P, Koob R, Amagai M, Gruber HJ, Drenckhahn D, Baumgartner W (2007). Imaging and force spectroscopy on desmoglein 1 using atomic force microscopy reveal multivalent Ca^{2+}-dependent, low-affinity trans-interaction. J Membr Biol 216, 83–92.
Wheelock MJ, Buck CA, Bechtol KB, Damsky CH (1987). Soluble 80-kd fragment of cell-CAM 120/80 disrupts cell-cell adhesion. J Cell Biochem 34, 187–202.
Wheelock MJ, Johnson KR (2003). Cadherins as modulators of cellular phenotype. Annu Rev Cell Dev Biol 19, 207–235.
Wilmanns C, Grossmann J, Steinhauer S, Manthey G, Weinhold B, Schmitt-Graff A, von Specht BU (2004). Soluble serum E-cadherin as a marker of tumour progression in colorectal cancer patients. Clin Exp Metastasis 21, 75–78.
Winter JN, Jefferson LS, Kimball SR (2011). ERK and Akt signaling pathways function through parallel mechanisms to promote mTORC1 signaling. Am J Physiol Cell Physiol 300, C1172–C1180.